BIOCHEMISTRY
including biophysical chemistry & molecular biology
Article

Biochemistry **2009,** *48,* 5365–5374 5365
DOI: 10.1021/bi9003155

Assembly and Stability of the Shiga Toxins Investigated by Electrospray Ionization Mass Spectrometry[†]

Elena N. Kitova,[‡] George L. Mulvey,[§] Tanis Dingle,[§] Igor Sinelnikov,[‡] Stefanie Wee,[§] Thomas P. Griener,[§] Glen D. Armstrong,[§] and John S. Klassen*,[‡]

[‡]*Department of Chemistry, University of Alberta, Edmonton, Alberta, Canada T6G 2G2, and* [§]*Department of Microbiology and Infectious Diseases, Faculty of Medicine, University of Calgary, Alberta, Canada T2N 4N1*

Received February 23, 2009; Revised Manuscript Received April 25, 2009

ABSTRACT: A systematic investigation into the assembly and stability of native and modified subunits of the Shiga toxins (Stx) *in vitro* is described. Analysis of the assembly of native and modified B subunits of Stx1 and Stx2 in solution, carried out using electrospray ionization mass spectrometry (ES-MS), suggests that the lower thermodynamic stability of the B subunit homopentamer of Stx2, compared to that of Stx1, is due to the presence of a repulsive interaction involving Asp70 of the Stx2 B subunit. In Stx1 B, the corresponding (spatially) residue is Arg. Using temperature-controlled ES-MS, it is shown that the Stx1 and Stx2 holotoxins exhibit differences in their resistance to temperature- and acid-induced dissociation. However, both Stx1 and Stx2 are fully assembled at pH >3.5 and 37 °C. This finding has several important biological implications. First, it argues against the likelihood that the difference in Stx1 and Stx2 toxicity arises from differential dissociation of the toxins during the intracellular trafficking steps of the cellular intoxication process. Second, it implies that the activation of the A subunits of Stx1 and Stx2 by enzymatic cleavage must occur while the A subunit is assembled with the B subunit homopentamer. It is, therefore, proposed that the differential toxicities of Stx1 and Stx2 reflect the relative efficiencies of intracellular activation of the A subunits.

The Shiga toxins (Stx)[1] 1 and 2 are bacterial enterotoxins produced by the enterohemorrhagic group of enterovirulant *Escherichia coli* (EHEC) (*1*). These organisms represent a subgroup of the shigatoxigenic or verotoxigenic *E. coli* (STEC or VTEC) and are isolated from human subjects experiencing hemorrhagic colitis and, occasionally, the hemolytic−uremic syndrome (HUS). Although numerous EHEC serotypes have been isolated from subjects experiencing hemorrhagic colitis, *E. coli* O157:H7 represents the predominant serotype in North America, Japan, and Europe. The Shiga toxins display classical AB_5 structures, in which a single A subunit (∼32 kDa) is associated with five identical B subunits (∼8 kDa) (*2*, *3*). The amino acid sequences of the A and B subunits of Stx1 and Stx2 are 52% and 60% identical, respectively (*4*, *5*). The A subunit is responsible for toxicity and acts by shutting down protein biosynthesis in target cells. The five B subunits assemble into a doughnut-shaped structure in which the central pore of this assembly hosts the C-terminus of the A subunit (*2*, *3*). The B_5 homopentamers contain multiple binding sites for a glycolipid (Galα1−4Galβ1−4glucosylceramide, Gb3), the natural Stx receptor located on the surface of target cells (*6*). Stx binding to the Gb3 receptor sequences initiates a chain of events leading ultimately to its internalization by endocytosis into the host cell (*7*). While multiple intracellular trafficking pathways may operate, the toxins are thought to move from the plasma membrane through the Golgi and endoplasmic reticulum (ER) to the cytosol. In the ER, the A subunit is cleaved into the A1 and A2 fragments (which remain bound through a disulfide bond) by proteases. Upon reduction, the A1 fragment is transported to the cytosol, where it acts on the 60S ribosomal subunit, blocking protein synthesis and causing cell death (*8*, *9*).

Despite the structural similarities suggested by X-ray analysis, Stx1 and Stx2 exhibit marked differences in biological activity; Stx2 being more potent than Stx1 *in vivo* and more closely associated with the most severe consequences of EHEC infections in humans whereas the opposite is true of their *in vitro* activities (*6*, *10*). The origin of the differential toxicities of Stx1 and Stx2 is not fully known but may arise from differences in receptor recognition (*11*), differences in their structure and stability which are not apparent in the X-ray crystal structures, or differences in their enzymatic activity. A recent comparative binding study showed that Stx1 and Stx2 exhibit similar affinities for the α-D-Gal*p*(1→4)-β-D-Gal*p*(1→4)-β-D-Glc*p* carbohydrate motif of Gb3 (*12*). Although not definitive, these results argue against

[†]This work was funded in part by the Natural Sciences and Engineering Research Council of Canada and the Alberta Ingenuity Centre for Carbohydrate Science.

*To whom correspondence should be addressed. Phone: (780) 492-3501. Fax: (780) 492-8231. E-mail: john.klassen@ualberta.ca.

[1]Abbreviations: Stx1 and Stx2, Shiga toxins type 1 and type 2; ES-MS, electrospray ionization mass spectrometry; EHEC, enterohemorrhagic group of enterovirulant *Escherichia coli*; STEC, shigatoxigenic *E. coli*; VTEC, verotoxigenic *E. coli*; HUS, hemolytic−uremic syndrome; ER, endoplasmic reticulum; FT-ICR/MS, Fourier transform ion cyclotron resonance mass spectrometry; nanoES, nanoflow ES.

Published on Web 04/28/2009

differential host cell recognition as underlying the differences in Stx1 and Stx2 biological activities. The results of a cell-free rabbit reticulocyte lysate assay failed to detect any differences in activity of the A subunits of Stx1 and Stx2 (*10*, *13*), suggesting that differential enzyme activity is not responsible for the toxicity differences. Recently, our laboratories undertook the first comparative study of the assembly of the Stx1 and Stx2 B subunits (*14*). The assembly of the B subunits of Stx1 and Stx2 under a variety of solution conditions was investigated using electrospray ionization mass spectrometry (ES-MS), a technique that is now widely used to probe the stoichiometry, stability, and dynamics of multiprotein complexes (*15*−*21*). Notably, this study revealed that the homopentamer of the Stx1 B subunit is thermodynamically more stable than the Stx2 B pentamer, under all conditions investigated, and raised the possibility that the differences in toxicity of Stx1 and Stx2 may be related to the differences in the stability of the holotoxins or the corresponding B subunit homopentamers (*14*).

Here, we describe the results of the first direct comparative study of the assembly and stability of native and modified subunits of the Shiga toxins (Stx) *in vitro*. Using ES-MS, the assembly and stabilities of the Stx1 and Stx2 holotoxins were investigated under a variety of solution conditions. Additionally, ES-MS measurements performed on a series of mutants of the Stx1 and Stx2 B subunits allowed the critical intersubunit interactions within the Stx B_5 homopentamers to be identified.

EXPERIMENTAL PROCEDURES

Toxins. Stx1 and Stx2 holotoxins were affinity purified using Synsorb-Pk as described previously (*22*, *23*). Reassembly of the holotoxins from their recombinant or purified subunits was accomplished according to the procedure described by Head et al.(*11*).

The coding sequences of the Stx1 and Stx2 B subunit genes were altered to introduce single and double point mutations. The following are the mutations introduced into the B subunits of Stx1 and Stx2: Stx1 B mutant **1** (Lys13Ala), Stx1 B mutant **2** -(Arg33Ala), Stx1 B mutant **3** (Arg69Ala), Stx1 B mutant **4** -(Lys13Asp), Stx1 B mutant **5** (Arg33Asp), Stx1 B mutant **6** -(Arg69Asp), Stx1 B mutant **7** (Lys08Ala), Stx1 B mutant **8** -(Asn35Ala), Stx1 B mutant **9** (Phe68Ala), Stx1 B mutant **10** -(Lys08Ala/Arg69Ala); Stx2 B mutant **11** (Glu09Ala), Stx2 B mutant **12** (Asp70Ala), Stx2 B mutant **13** (Glu09Arg), Stx2 B mutant **14** (Asp70Arg).

The mutated Stx1 B genes were cloned into pVERO (*25*). The plasmids containing the mutated Stx1 B subunit gene sequences were transformed into the BL21-AI *E. coli* expression strain according to the QIAGEN transformation protocol. Next, single colonies of mutants **1**−**3** and **6**−**10** were grown, with shaking (200 rpm), in 20 mL of $LB_{carb100}$ overnight at 37 °C. These cultures were then diluted into 1 L of $LB_{carb100}$ and incubated at 37 °C, with shaking (200 rpm), until an OD_{600} of between 0.6 and 0.9 was reached. The expression of the mutant Stx1 B subunits was induced by adding 0.2% L-arabinose to the cultures for 3 h. The cultures were next treated with 0.1 mg/mL polymyxin B sulfate for 30 min at 37 °C. These polymyxin-treated cultures were centrifuged at 7000 rpm for 10 min at 4 °C, and the mutated Stx1 B subunits were affinity purified from the resulting cell-free culture supernatant solutions using Synsorb-Pk. Mutant **5** was purified by a combination of ultrafiltration and size exclusion chromatography while mutant **4** could not be isolated. By contrast, the Stx2 B subunit mutants **11**−**14** were cloned into the pBAD/His vector (Invitrogen Canada Inc., Burlington, Ontario). The plasmids were subsequently transformed into the LMG194 *E. coli* expression strain according to the QIAGEN transformation protocol. Next, single colonies of each transformant were grown, with shaking (200 rpm), in 20 mL of LB_{amp100} overnight at 37 °C. These cultures were then diluted into 1 L of LB_{amp100} and incubated at 37 °C, with shaking (200 rpm), until an OD_{600} of between 0.6 and 0.9 was reached. The expression of the mutant Stx2 B subunits was induced by adding 0.0002% L-arabinose to the cultures for 3 h. The mutant Stx2 B subunits were polymyxin-treated and purified using Synsorb-Pk as described for the mutant Stx1 B subunits. All purified mutant subunits were dialyzed against 50 or 100 mM ammonium acetate (pH 7) and stored at −20 °C.

Carbohydrates. The trisaccharide αTal[αAbe]αMan (M_{rep}) and the trivalent Pk analogue (**L**), a specific ligand for Stx1 and Stx2, were donated by Prof. D. R. Bundle (University of Alberta). Aqueous stock solutions of M_{rep} and of **L** were prepared at concentrations of 1 mM.

Mass Spectrometry. All MS measurements were performed using a modified Apex II 9.4 T FT-ICR/MS (Bruker, Billerica, MA) equipped with a temperature-controlled nanoflow ES (nanoES) device (*26*) that allows the solution temperature to be varied from 0 to 60 °C. The ES solutions were prepared by thawing the stock solutions at room temperature and diluting an aliquot of the B subunit to a final concentration of 50 μM with aqueous ammonium acetate. The ES solutions were allowed to stand for at least 10 min prior to acquiring mass spectra in order to establish an equilibrium distribution of the different multimeric states of the A and B subunits. Mass spectra measured at longer times were found to be indistinguishable from those measured at ∼10 min. NanoES tips, with an outer diameter of ∼5 μm, were pulled from aluminosilicate or borosilicate tubes (1 mm o.d., 0.68 mm i.d.) using a P-2000 micropipet puller (Sutter Instruments, Novato, CA). A platinum wire, inserted into the other end of the nanoES tip, was used to establish electrical contact with the nanoES solution. A potential of ±(600−800) V was applied to the platinum wire in the nanoES tip in order to spray the solution. The tip was positioned 1−2 mm from a stainless steel sampling capillary using a microelectrode holder. Typical solution flow rates were ∼20 nL/min. Charged droplets and ions emitted by the nanoES tip were introduced into the vacuum chamber of the mass spectrometer through a heated stainless steel sampling capillary (0.43 mm i.d.) maintained at an external temperature of 66 °C. The gaseous ions sampled by the capillary (±48 V) were transmitted through a skimmer (±4 V) and accumulated for 2−5 s in an rf hexapole (±600 V p-p). The ions were subsequently ejected from the hexapole and injected at ±2700 V into the bore of the superconducting magnet, decelerated, and introduced into the ion cell. The typical base pressure for the instrument was $\sim 5 \times 10^{-10}$ mbar. Data acquisition was performed using the XMASS software (version 5.0). The time-domain signal consisted of the sum of 50−100 transients containing 128 K data points per transient.

RESULTS AND DISCUSSION

Assembly of Stx B Subunits. A previous ES-MS study of the assembly of the B subunits of Stx1 and Stx2 *in vitro* revealed significant differences in the stability of the B_5 homopentamers of the two toxins (*14*). These differences are illustrated in Figure 1,

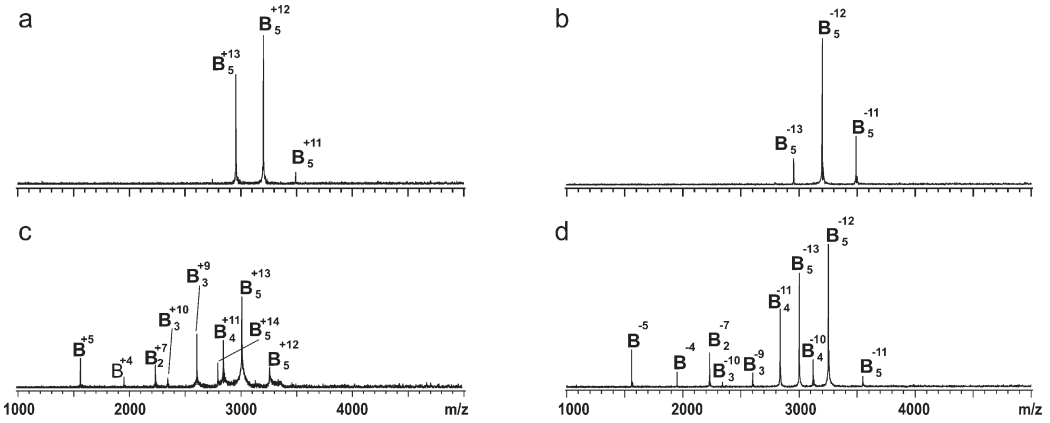

FIGURE 1: NanoES mass spectra acquired in positive and negative ion modes for aqueous solutions of (a, b) Stx1 B and (c, d) Stx2 B, at a subunit concentration of 50 μM. All solutions contained 20 mM ammonium acetate (pH 7) at 25 °C.

where ES mass spectra obtained in both positive and negative ion mode for solutions of B subunits of Stx1 (MW 7686 Da for monomer) and Stx2 (MW 7815 for monomer) at a concentration of 50 μM in 20 mM ammonium acetate are shown. According to the MS data, the fraction of homopentamer in solution differs considerably for the two B subunits under these conditions: the B subunit of Stx1 exists exclusively as the homopentamer, while the B subunit of Stx2 exists simultaneously as monomer (B), dimer (B_2), trimer (B_3), tetramer (B_4), and pentamer (B_5). Due to possible differences in the ES-MS response factors (ionization and detection efficiencies), the relative abundance of the Stx2 B subunit multimers detected by ES-MS may not accurately reflect solution composition. Furthermore, in-source (gas phase) dissociation of the B subunit multimer ions and nonspecific self-association of monomers and multimers during the ES process may influence the relative abundance of the Stx2 B subunit monomer and multimers reflected in the mass spectra. It was previously suggested that in-source dissociation of the Stx2 B subunit multimer ions does not occur appreciably in ES-MS analysis (*14*). To further test whether the Stx2 B subunit multimer ions are kinetically stable during ES-MS analysis, mass spectra were acquired for a solution of Stx2 B subunits containing 5 mM imidazole. The presence of imidazole has been shown to minimize the occurrence of in-source dissociation for noncovalent protein complexes (*27*). Notably, the addition of imidazole did not significantly alter the relative abundance of monomer and multimer ions (data not shown). This result argues against the occurrence of in-source dissociation during ES-MS analysis of the Stx2 B pentamer.

To test whether nonspecific self-association of Stx2 B subunits occurs during the ES process, the reporter molecule method was used (*28*). Briefly, a reporter molecule (M_{rep}) is added to the solution at elevated concentration, and the distribution of M_{rep} molecules bound nonspecifically to the protein ions is compared. Because nonspecific protein complexes are formed later in the ES process (from older, more concentrated droplets), they undergo greater nonspecific binding with M_{rep} compared to monomer and specific multimers (*28*). Shown in Figure 2a is an illustrative ES mass spectrum acquired for solutions of the Stx2 B subunit (50 μM) and trisaccharide αTal[αAbe]αMan (100 μM), which served as M_{rep}. Ions corresponding to the nonspecific attachment of one or more molecules of M_{rep} to monomer, dimer, and trimer ions of the B subunit are identified in the mass spectrum. Shown in Figure 2b are the normalized distributions of bound M_{rep} to monomer, dimer, and trimer ions, as determined from the mass spectrum. Importantly, the distributions of M_{rep} bound nonspecifically to monomer and trimer are similar but distinct from the distribution determined for dimer, which undergoes more extensive nonspecific binding with M_{rep}. These results imply that the trimer ions arise predominantly from solution, while nonspecific association of monomer contributes appreciably to the signal for the dimer ions (at the concentration investigated). Because of the suppression of the tetramer and pentamer ions by M_{rep}, an unexpected finding, it was not possible to establish whether nonspecific subunit association contributes appreciably to the tetramer and pentamer ion signal under these conditions. While it may not be possible to quantify the distribution of Stx2 B subunit monomer and multimers in solution due to nonspecific subunit association and, presumably, differences in response factors, the ES-MS data do, nevertheless, provide clear evidence that the B subunit homopentamer of Stx2 is thermodynamically less stable than that of Stx1 under the conditions investigated.

Assembly of Mutant Stx B Subunits. Analysis of the crystal structures of Stx1 (*2*) and Stx2 (*3*) reveals two common inter-B subunit salt bridges: Glu65-Lys13 and Arg33-Asp18 (Stx1); Glu64-Lys12 and Arg32-Asp17 (Stx2). A third putative ionic interaction can be identified for both homopentamers: a stabilizing salt bridge Glu10-Arg69 (Stx1) and a repulsive (destabilizing) ionic interaction Asp70-Glu09 (Stx2). It was suggested in an earlier study that the difference in the nature of the third ionic interaction is, at least in part, responsible for the difference in thermodynamic stability of the B_5 homopentamers of Stx1 and Stx2 (*14*). Differences in intersubunit hydrogen bonds and hydrophobic forces may also contribute to the difference in stability of the B_5 homopentamers. A mutagenesis study was carried out to probe more directly the role of specific intersubunit interactions in stabilizing (or destabilizing) the B_5 homopentamers of Stx1 and Stx2. A series of mutants of the B subunits of Stx1 and Stx2 were produced, and their tendency to assemble into pentamers was evaluated by ES-MS. To assess the importance of the salt bridges in the assembly of Stx1 B_5, six mutants (**1**−**6**), in which the basic residues of the three putative salt bridges were replaced with Ala or Asp, were prepared. Shown in Figure 3 are ES mass spectra, acquired in both positive and negative ion mode, for mutants **1**−**3** and **6** at a subunit concentration of 50 μM (at 25 °C). Neither the replacement of Lys13 (**1**) nor Arg69 (**3**) with Ala resulted in the appearance of ions other than the B_5 homopentamer ions (Figure 3a,b,e,f). Taken on their own, these results suggest that neither residue (nor the putative ionic interactions) is critical for homopentamer formation under the

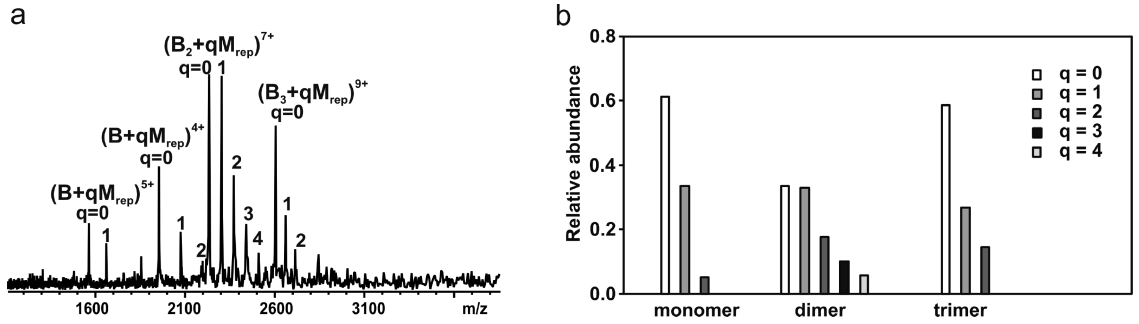

FIGURE 2: (a) NanoES mass spectrum for an aqueous solution of Stx2 B (50 μM) and M_{rep} (100 μM), with 20 mM ammonium acetate (pH 7) at 25 °C. (b) Distribution of M_{rep} bound nonspecifically to B^{n+}, B_2^{n+}, and B_3^{n+} ions, as determined from the mass spectrum in (a).

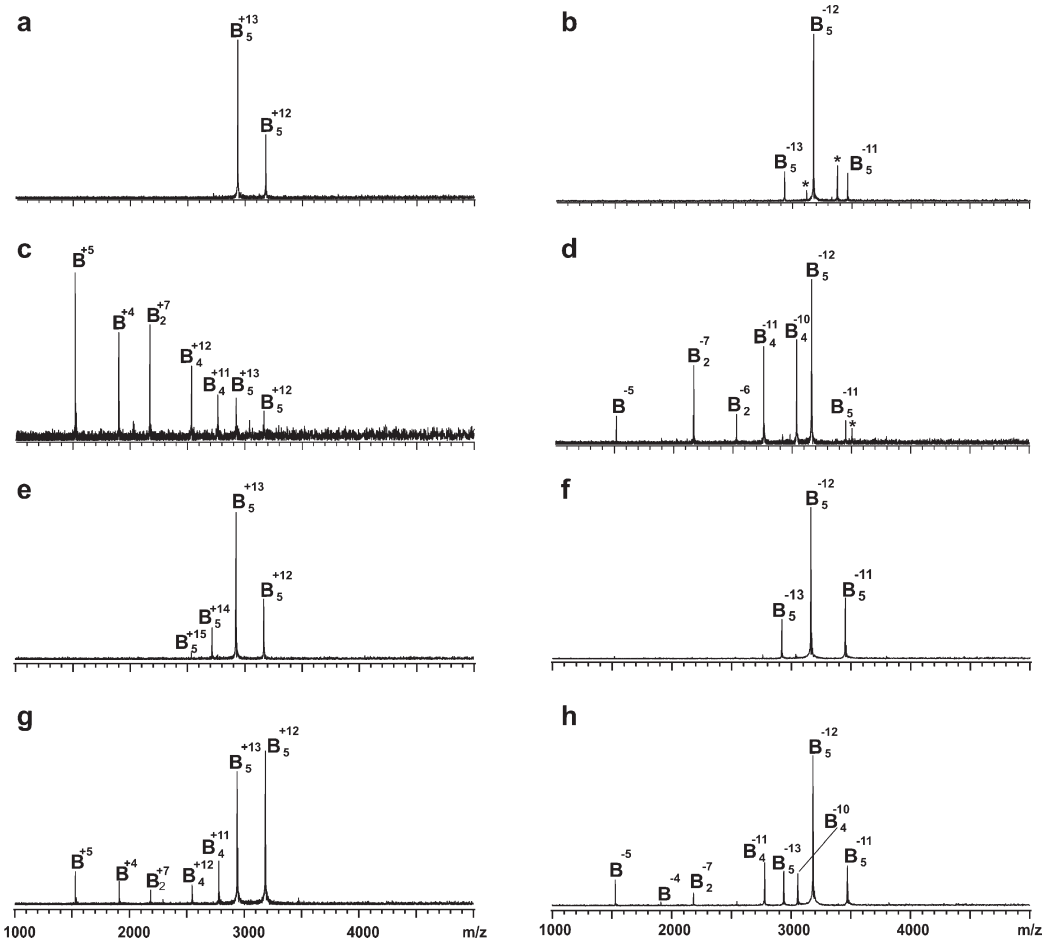

FIGURE 3: NanoES mass spectra obtained positive and negative ions modes for aqueous solutions of mutants of the Stx1 B subunit at a subunit concentration of 50 μM: (a, b) Lys13Ala (**1**); (c, d) Arg33Ala (**2**); (e, f) Arg69Ala (**3**); (g, h) Arg69Asp (**6**). All solutions contained 20 mM ammonium acetate (pH 7) at 25 °C.

solution conditions investigated. In contrast, replacement of Arg33 in the Stx1 B subunit with Ala (**2**) significantly destabilized the homopentamer and resulted in the appearance of B, B_2, and B_4 ions in the mass spectra (Figure 3c,d). Interestingly, the distribution of B subunit species for this mutant depended significantly on the polarity of the measurement, with a much higher fraction of pentamer observed in negative ion mode. The difference in the distributions observed in positive and negative ion modes likely reflects differences in their relative ionization efficiencies. Mass spectra obtained for mutant **4**, where Lys13 was replaced with Asp, showed only the presence of monomer (data not shown). This result is consistent with the observation that this mutant could not be isolated by affinity chromatography since the monomeric form of the B subunit is not expected to be efficiently retained by the affinity column. Similarly, mutant **5** could not be isolated by affinity chromatography, suggesting that replacement of Arg33 with aspartic acid results in the failure of these mutated B subunits to self-assemble into multimers. While it is likely that introducing a repulsive ionic interaction (Glu65-Asp13 or Asp33-Asp18) significantly destabilizes the homopentamer making affinity purification impossible, there is also the possibility that the mutations perturb binding between the B subunits and the Pk trisaccharide. Replacement of Arg69 with Asp (mutant **6**) destabilizes the pentamer, resulting in the appearance of B, B_2, and B_4 ions in the mass spectra, although the B_5 ions are the dominant ions detected (Figure 3g,h). It is worth noting that the mass spectra obtained for mutant **6**, particularly in negative ion mode, are similar to those obtained

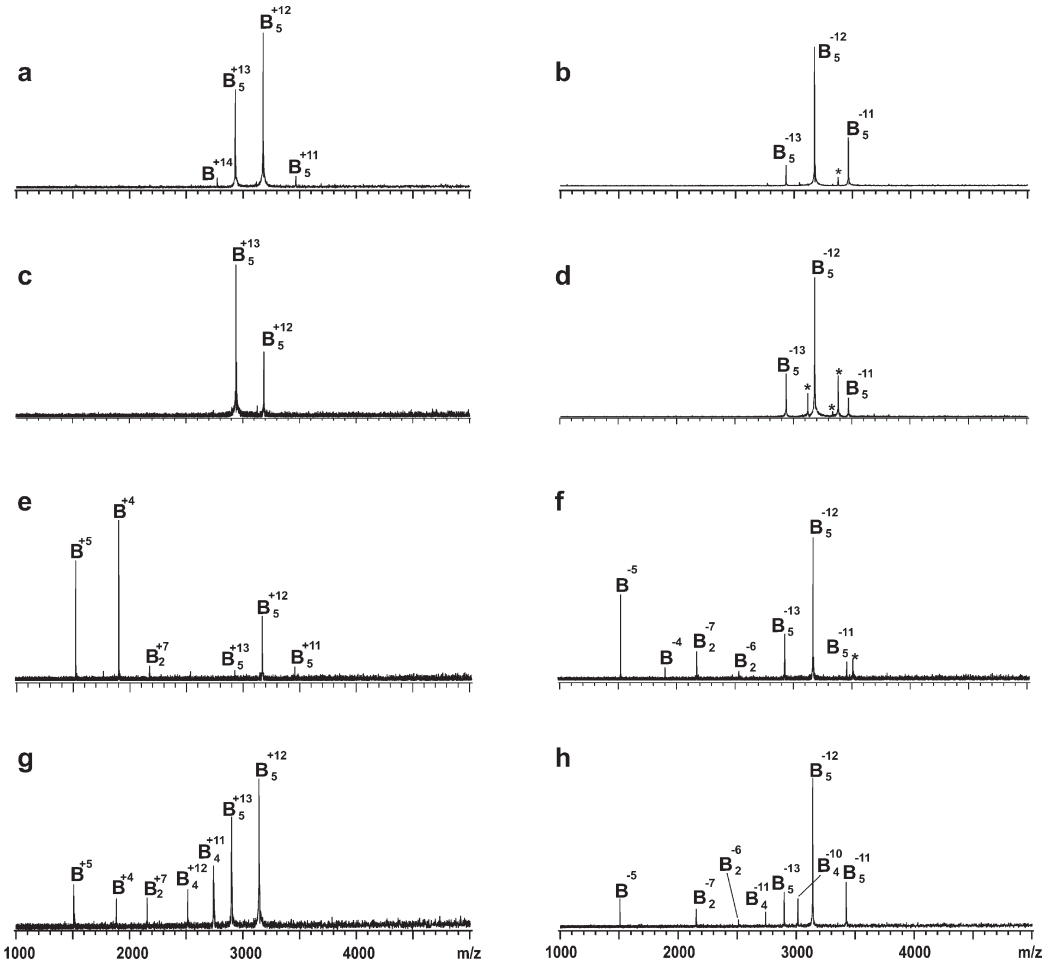

FIGURE 4: NanoES mass spectra obtained for aqueous solutions of Stx1 B mutants at a subunit concentration 50 μM: (a, b) Lys08Ala (**7**); (c, d) Asn35Ala (**8**); (e, f) Phe68Ala (**9**); (g, h) Arg69Ala, Lys08Ala (**10**). All solutions contained 20 mM ammonium acetate (pH 7) at 25 °C. Impurities are indicated by *.

for the native Stx2 B subunit under similar solution conditions. This finding supports the hypothesis that the different stabilities of the B_5 assemblies of Stx1 and Stx2 arise from the difference in a single ionic intersubunit interaction.

To assess the role of hydrogen bonds in stabilizing the pentamer, single point mutations at Lys08, Asn35, and Phe68 with Ala (**7**−**9**) were prepared. A double point mutant (**10**), in which both Lys08 and Arg69 were replaced with Ala, was also prepared. According to the crystal structure of Stx1 B_5 (*2*), Lys08, Asn35, and Phe68 engage in intra- and intersubunit H-bonds. The side chain of Lys08 is buried within the subunit and may form hydrogen bonds with Thr49, Val09, and Gly47 located in the same subunit. The side chain of Asn35 interacts with Tyr14 on an adjacent subunit, while Phe68 interacts with Thr12 and Gln44 on a neighboring subunit. Shown in Figure 4 are illustrative ES mass spectra acquired in positive and negative ion mode for these four mutants. According to the mass spectra, mutants **7** and **8** exist almost entirely as homopentamers under the solution conditions investigated (Figure 4a−d). These results suggest that neither Lys08 nor Asn35 is involved in H-bonds critical for assembly. In contrast, mutation at Phe68 (mutant **9**) results in a significant loss in the stability of the homopentamer (Figure 4e,f), which suggests that the putative H-bonds identified for this residue in the crystal structure are important for assembly. Interestingly, while the individual mutation of Arg69 or Lys08 to Ala did not result in any detectable decomposition of the corresponding pentamers, the double mutation Arg69Ala/Lys08Ala (**10**) led to a noticeable decrease in stability (Figure 4g,h). This likely reflects the cumulative destabilizing effect of the two mutations.

According to the crystal structures, the residues Lys07, Lys12, Arg32, Asn34, and Phe67 of Stx2 B are the counterparts of residues Lys08, Lys13, Arg33, Asn35, and Phe68 in Stx1 B. The spatial location of these residues within the subunits and their intra- and intermolecular contacts are very similar. Consequently, these residues are expected to play similar roles in stabilizing the homopentamers of Stx1 and Stx2. A notable difference in the primary structure of Stx1 and Stx2 B subunits is in the residues at position 69 of Stx1 and 70 of Stx2. In Stx1 B, residue 69 is Arg, while in Stx2 B the corresponding (spatially) residue is Asp. As discussed above, it is possible that the difference in stability of the B subunit homopentamers of Stx1 and Stx2 is due, at least in part, to the presence of the repulsive ionic interaction between Asp70 and Glu09 in the Stx2 B subunit. To further test this hypothesis, a series of single point mutants of the Stx2 B subunit, in which residues Glu09 and Asp70 were substituted with Ala (**11**, **12**) or Arg (**13**, **14**) were prepared. Shown in Figure 5 are illustrative ES mass spectra acquired in positive ion mode for the four Stx2 B mutants. Deletion of the putative repulsive interaction through mutation of Asp70 to Ala (**12**) or Arg (**14**) resulted in a measurable increase in the relative abundance of homopentamer (Figure 5a,b), compared to the native B subunit. Notably, mutant **14** is detected almost exclusively as the homopentamer, behavior that is more consistent

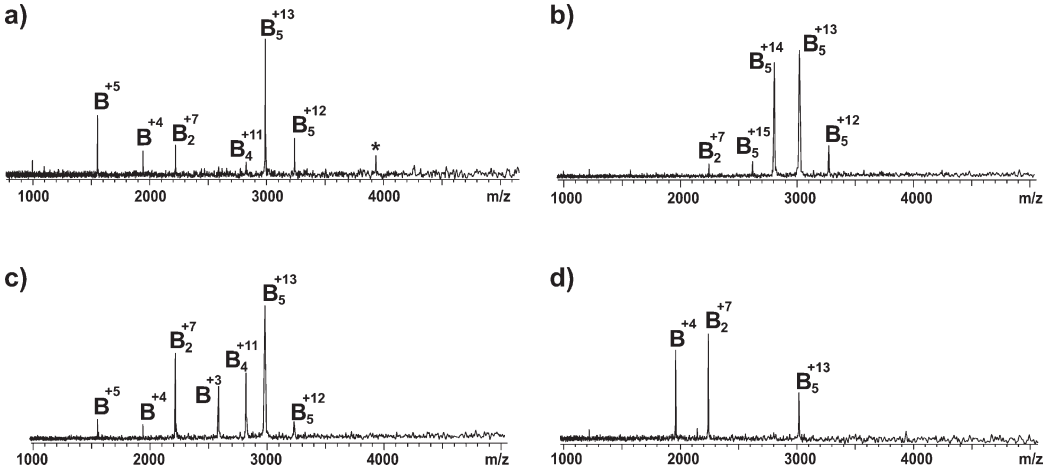

FIGURE 5: NanoES mass spectra obtained for aqueous solutions of Stx2 B mutants at a subunit concentration of 50 μM: (a) Asp70Ala (**12**); (b) Asp70Arg (**14**); (c) Glu09Ala (**11**); (d) Glu09Arg (**13**). All solutions contained 20 mM ammonium acetate (pH 7) at 25 °C. Impurities are indicated by *.

with Stx1 B than Stx2 B. In contrast, replacement of residue Glu09 with Ala (**11**) did not lead to any appreciable increase in the relative abundance of homopentamer (compared to that observed for Stx2 B), while replacement with Arg (**13**) led to a profound decrease in the relative abundance of the homopentamer. Taken together, the ES-MS data obtained for the native and mutant B subunits of Stx1 and Stx2 strongly suggest that a repulsive interaction involving Asp70 destabilizes the homopentamer of Stx2 B. However, Glu09 does not appear to be involved in this destabilizing interaction.

Exchange of Stx B Subunits. ES-MS was also used to evaluate the extent to which the B subunits of Stx1 and Stx2, as well as the mutant B subunits, can assemble into heterocomplexes. Shown in Figure 6 are ES mass spectra acquired in positive ion mode for solutions containing B subunits of both Stx1 and Stx2 at molar ratios 4.5:5.5 and 4:1. The mass spectra acquired for mixtures of the two subunits reveal the presence of mixed pentamers. This result indicates that subunit exchange readily occurs on the time scale of the measurements (~5−10 min). Importantly, the relative distribution of homo- and heteropentamers at equilibrium closely reflects the relative molar concentrations of the Stx1 and Stx2 B subunits in solution. For example, at a molar ratio of 4:1 the dominant heteropentamer ions detected correspond to $(B_{Stx1})_4(B_{Stx2})$. The occurrence of subunit exchange is not unexpected given that, according to crystallographic data, the B subunits of Stx1 and Stx2 have nearly identical higher order structures. However, the enhancement in the stability of heteropentamers, compared to Stx2 B_5, was surprising. The greater stability of the heteropentamer is consistent with the replacement of the repulsive ionic interaction involving Asp70 (which is present in Stx2 B_5) with a stabilizing ionic interaction between Arg69 in Stx1 B and an unidentified residue in the neighboring Stx2 B subunit. Interestingly, the mutant Stx1 B subunits were also found to readily assemble with native the Stx1 B subunit to form stable heteropentamers (data not shown). This finding suggests that the high order structure of the Stx1 B subunit was not significantly disturbed by the selected mutations.

Assembly of Stx1 and Stx2 Holotoxins. Temperature-controlled ES-MS was used to carry out the first direct comparative study of the stabilities of the Stx holotoxins at different solution temperatures and pH. Shown in Figure 7 are representative ES mass spectra obtained in positive ion mode for solutions of native Stx1 or Stx2 at nominal AB_5 concentrations of 4 μM at 35 °C and pH 7, 4, and 3. At pH 7, only ions corresponding to the intact holotoxin, i.e., AB_5^{n+}, were detected for the solution of Stx2 (MW 72230 Da) (Figure 7b). Abundant B_5 (MW 38430 Da) and AB_5 (MW 70622 Da) ions were detected for the solution of Stx1; B_{10} ions were also detected, albeit at low abundance (Figure 7a). The B_{10} ions likely result from nonspecific association of two B_5 complexes during the ES process, although this remains to be confirmed. It is interesting to note that in a recent ES-MS study of Stx1 at pH 7, in addition to AB_5 ions, abundant B and B_5 ions were also detected (*29*). The origin of the B and B_5 ions, however, was not discussed. Importantly, ions corresponding to free A subunit (i.e, A^{n+}) were not detected in either the present or the previous study, suggesting that the B_5 ions do not originate from the dissociation of the AB_5 holotoxin in the stock or ES solutions nor in the gas phase (in-source dissociation). Rather, partial dissociation of the Stx1 AB_5 assembly in cell-free culture supernatant solution may occur prior to affinity purification. As described above, the B subunit of Stx1 readily assembles into homopentamer in solution, and it is known to bind strongly to the Synsorb-Pk affinity column (*22*). It is also possible that the Stx1 B subunit gene is overexpressed in *E. coli* and it is copurified with holotoxin. The absence of free B subunits in the mass spectrum obtained for Stx2 does not, in itself, preclude the possibility that the Stx2 B subunit gene is similarly overexpressed in *E. coli* or that the AB_5 complex is similarly prone to partial dissociation at low concentrations. As shown above and elsewhere (*14*), at low concentrations, the Stx2 B subunits exist preferentially as monomer and dimer, which are not efficiently retained on the affinity column.

At pH 4, AB_5 ions were detected for both Stx1 and Stx2 (Figure 7b,e). In the case of Stx2, these are the only protein ions present, indicating that the holotoxin is stable at this pH and temperature. For Stx1, B and B_2 ions, in addition to AB_5 and B_5 ions, are detected. However, the absence of A ions indicates that the holotoxin is stable at this pH and temperature and that the B and B_2 ions originate from the disassembly of the B_5 homopentamer, which was shown to dissociate at pH ~4 and less (*30*).

At pH ~3 (Figure 7c,f), AB_5 ions of Stx1 and Stx2 were either present in low abundance or completely absent in the mass spectra. In the case of Stx1, B, B_2, and B_3 ions, along with free A ions, were detected. The appearance of B_3 ion at pH ~3 (compared to pH 4 where these ions are largely absent) is

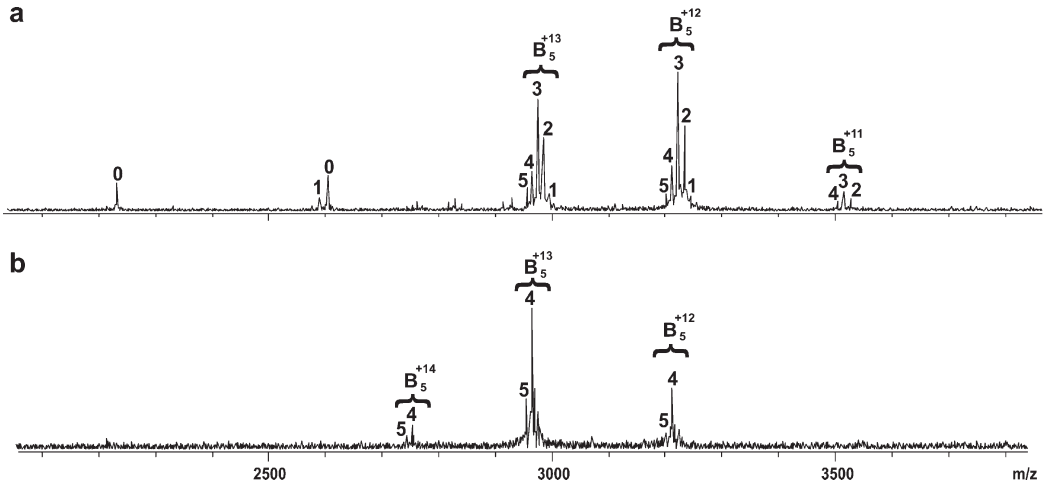

FIGURE 6: NanoES mass spectra obtained for aqueous solutions of (a) Stx1 B and Stx2 B at molar concentration ratio 55 to 45 and (b) Stx1 B and Stx2 B at molar concentration ratio 4 to 1. All solutions contained 20 mM ammonium acetate (pH 7) at 25 °C. The numbers above each peak correspond to the number of Stx1B subunits contained within each pentamer.

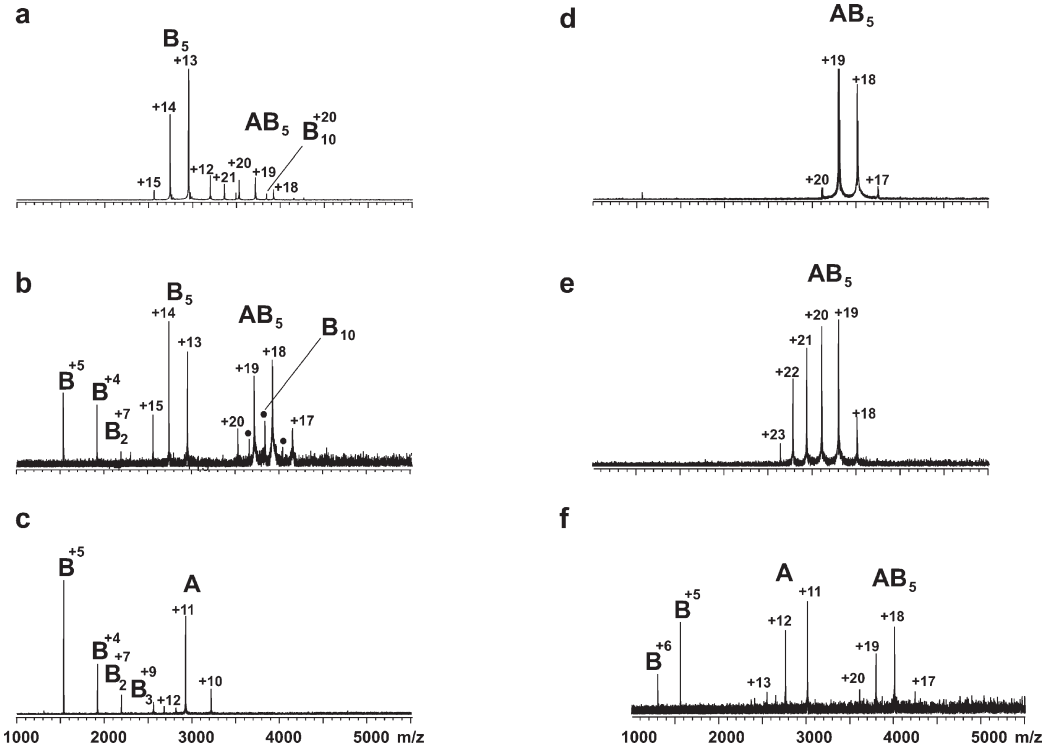

FIGURE 7: NanoES mass spectra of aqueous ammonium acetate (10 mM) solutions of 4 μM Stx1 at (a) pH 7, (b) pH 4, (c) pH 3, and a solution temperature of 35 °C or of 4 μM Stx2 at (d) pH 7, (e) pH 4, (f) pH 3, and a solution temperature of 35 °C.

attributed to the increased B subunit concentration resulting from the disassembly of the holotoxin. For Stx2, only B and A ions were detected, in addition to assembled AB_5 ions. The absence of multimeric B subunits is consistent with the results of a previous study that showed that the B subunit exists exclusively as monomer at pH < 4 (*14*). Notably, complexes of the A subunit bound to B subunit multimers smaller than pentamer were not observed. This indicates that dissociation of the AB_5 assembly proceeds only by the loss of the A subunit whereas tight binding of individual B subunits to adjacent subunits prevents their dissociation from the complex. Interestingly, narrow charge state distributions (charge states $+10$ to $+13$) were observed for the free A subunits of Stx1 and Stx2, indicating that the A subunits are lost from the holotoxins in their native form, or at least as a compact structure, at this pH (*31*). Additionally, the charge state distributions of the AB_5 ions of Stx1 and Stx2 were found to be relatively insensitive to pH (over the range investigated), consistent with the preservation of their native structure under the solution conditions investigated. Based on these results, a two-step acid-induced dissociation mechanism for the Stx1 and Stx2 holotoxins is proposed: the loss of the folded A subunit, followed by the dissociation of the homopentamer.

The influence of pH on the stability of Stx1 and Stx2 holotoxins was investigated in more detail over a range of solution temperatures (20−60 °C). A series of solutions of Stx1 or Stx2, where the pH varied from 7 to 2.6, were assayed at different temperatures using ES-MS. The appearance of signal in the mass spectra corresponding to free A subunit served to identify the onset of holotoxin dissociation at a given temperature. Notably, this onset was found to occur within a narrow pH

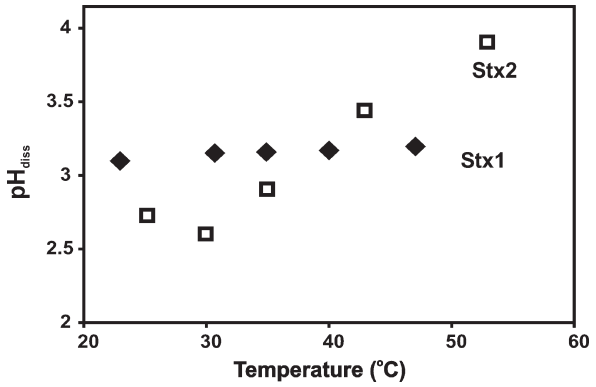

FIGURE 8: pH_{diss} values of Stx1 and Stx2 determined as a function of solution temperature. The uncertainty in the pH_{diss} values is 0.1 pH unit.

range, ~0.1. The average values of pH where the onset of dissociation of a given holotoxin was observed (pH_{diss}) are plotted versus temperature in Figure 8. At pH >4, no dissociation of either holotoxin was detected at solution temperatures up to 60 °C. For Stx1, the value of pH_{diss} showed very little temperature dependence and was centered at ~3.2. In contrast, pH_{diss} for Stx2 varied significantly with temperature. At temperatures <30 °C, the value of pH_{diss} was ~2.6; at >30 °C, pH_{diss} increased nearly linearly with temperature. These results reveal for the first time that the forces responsible for the assembly of the Stx1 and Stx2 holotoxins are different under the solution conditions investigated. Curiously though, Stx1 and Stx2 exhibit approximately the same pH_{diss} value at physiological temperature.

It should be noted that the results of the pH−temperature study do not fully agree with the results of a previous study by Tesh et al. (*10*) that suggested Stx2 is more heat and pH stable than Stx1. In that earlier study, the stability of the holotoxins was assessed from changes in verocytoxicity of the toxins following incubation at different temperatures and pH. Importantly, prior to performing the assays, the toxin solutions were chilled and neutralized (pH 7.5). The reason for the discrepancy between the findings of this earlier study and the present work is not fully understood but may be related in part to the differential ability of the A and the B subunits of Stx1 and Stx2 to reassemble prior to the cytotoxicity assay. Regardless, the results of the ES-MS assay, which provide direct insight into the assembly of the holotoxins under a given set of conditions, would seem to offer more reliable insight into the relative stabilities of the toxins.

A significant finding of the pH−temperature study is that both Stx1 and Stx2 are fully assembled at pH >3.5 and 37 °C. It follows that both Stx1 and Stx2 are stable under the weakly acidic conditions experienced in the endosomes (early endosomal pH is ~6; late endosomal pH is ~5 (*32*)). Consequently, it is unlikely that the difference in Stx1 and Stx2 toxicity arises from differential dissociation of the toxins during the intracellular trafficking steps of the cellular intoxication process. This finding has important implications for the mechanism of activation of the A subunits. It is concluded that the activation of the A subunits of Stx1 and Stx2 by enzymatic cleavage must occur while the A subunit is assembled with the B subunit homopentamer. It is, therefore, possible that the differential toxicities of Stx1 and Stx2 reflect the relative efficiencies of activation of the A subunits. Our laboratory is currently investigating this possibility.

Composition of Stx1 Preparations. Regardless of its origin, the presence of excess B subunit in the Stx1 preparations has potential implications for comparative toxicity studies employing Stx1 and Stx2 and might also explain the lower toxicity of Stx1 in *E. coli* O157:H7 infections. To our knowledge, the relative abundance of AB_5 and B_5 present within a given Stx1 sample has not heretofore been investigated. Because the response factors for the AB_5 and B_5 ions may be very different, *vide infra*, their relative abundance in the Stx1 preparations can not be reliably determined directly from the ES mass spectrum. Instead, an indirect method, based on specific ligand binding to Stx1 AB_5 and B_5, was used to establish their relative abundance. Briefly, to establish the total concentration of a given protein in solution ($[P]_o$), a ligand with known affinity (K_a) is added at a known concentration ($[L]_o$). The concentration ratio of bound to unbound protein at equilibrium ([PL]/[P] = R) is taken to be equal to the intensity (I) ratio of the corresponding bound and unbound protein ions ($R = I_{PL}/I_P$), as determined from the ES mass spectrum (*33*). From the known $[L]_o$, K_a, and R values, it is possible to calculate $[P]_o$ using eq 1 (*33*):

$$[P]_o = \frac{(1+R)([L]_o K_a - R)}{RK_a} \quad (1)$$

The specific ligand chosen for the present analysis was a trivalent Pk analogue (**L**) which has an affinity for the Stx1 B pentamer of 1.1×10^5 M^{-1} (*12*). The structure of **L** is given in Figure 9a, along with an illustrative mass spectrum acquired for a solution of Stx1 (0.8 mg/mL) and **L** (6 μM) at 25 °C. Ions corresponding to both unbound B_5 and AB_5 and B_5 and AB_5 bound to a single molecule of **L** were detected. The fractions of bound B_5 and AB_5 are identical (Figure 9b), consistent with identical affinities for **L**. From the measured R value and the known K_a and $[L]_o$ values, $[P]_o$ was determined. Because both B_5 and AB_5 bind to **L**, $[P]_o$ represents the total concentration of binding sites for **L**, which is related to the initial concentrations, $[B_5]_o$ and $[AB_5]_o$, by the expression:

$$[P]_o = (m_{B5}/M_{B5} + m_{AB5}/M_{AB5})/V \quad (2)$$

where m_{B5} and m_{AB5} are the masses of dissolved B_5 and AB_5, respectively, M_{B5} and M_{AB5} are the molar masses of B_5 and AB_5, respectively, and V is the solution volume. From $[P]_o$ and the known total mass (m) of dissolved protein (where $m = m_{B5} + m_{AB5}$), the mass (and concentration) of the B_5 and AB_5 species can be calculated. Following this procedure, B_5 was found to make up approximately 5% of the Stx1 sample by weight. The error in the holotoxin molar concentration caused by the presence of the B subunit therefore corresponds to ~10%, too small an amount, within experimental error, to explain the lower toxicity of Stx1 holotoxin preparations in mouse challenge experiments, *vide infra*. This result also indicates that, under the experimental conditions used for the binding measurements, the response factors for the B_5 ions are approximately 5 times larger than for the AB_5 ions.

Efforts to remove the B subunit from the Stx1 samples using gel filtration or membrane filters were found to be generally ineffective. It was, however, possible to minimize the amount of free B pentamer in the preparations by recombining free A and B subunits, which were initially separated and purified, at the appropriate molar ratios. Shown in Figure 10 are mass spectra acquired for solutions of recombined Stx1 and Stx2 at pH 7 and 25 °C. Notably, for both toxins, the AB_5 ions are the only protein ions detected at pH 7. These results indicate that recombining the A and B subunits of Stx1 is an effective way to reduce the

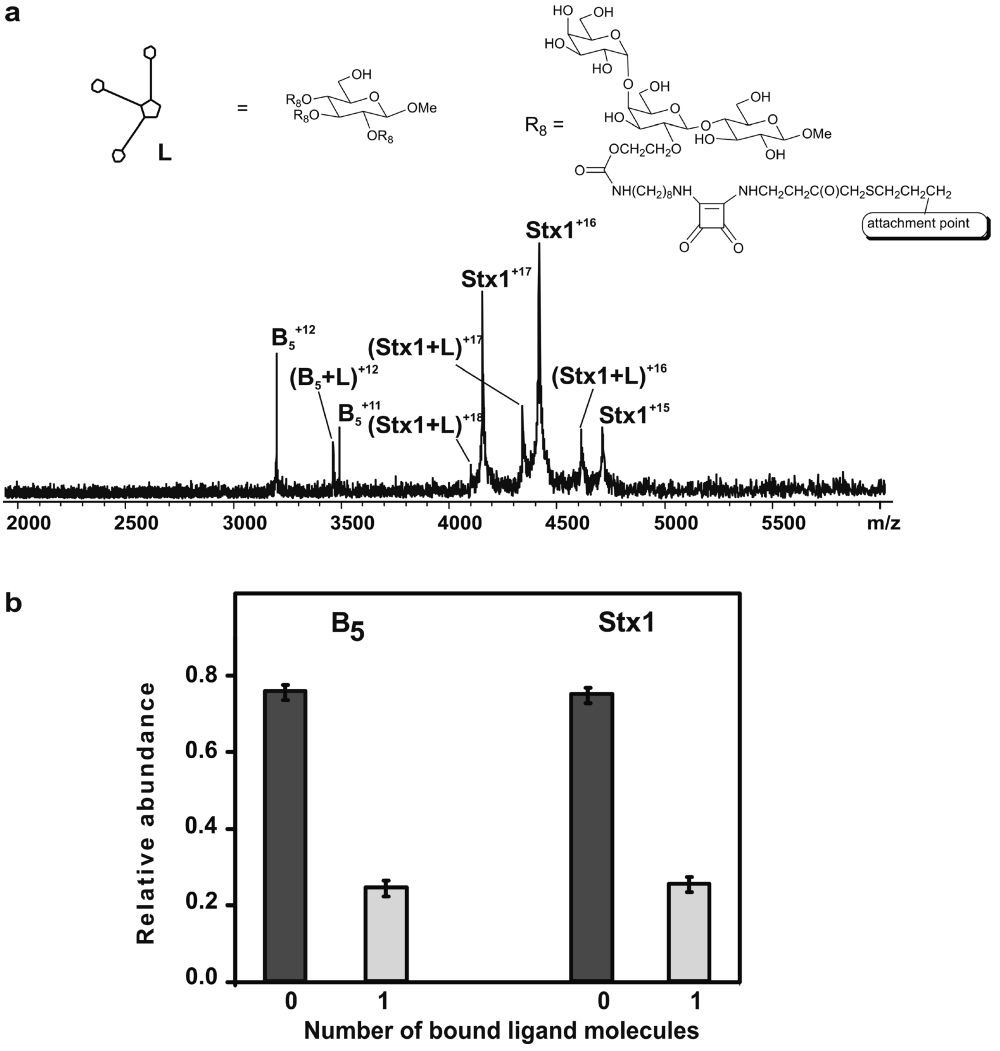

FIGURE 9: (a) NanoES mass spectrum of aqueous ammonium acetate (10 mM, pH 7) solution of 12.5 μM of Stx1 and 6 μM **L** at 25 °C. (b) Distributions of **L** bound to B_5 and Stx1 as determined from the mass spectrum shown in (a).

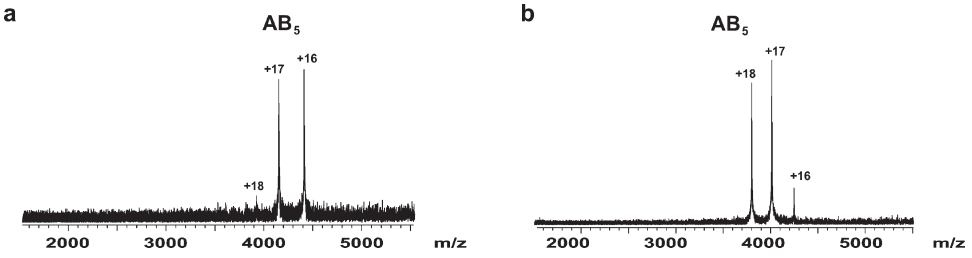

FIGURE 10: NanoES mass spectra of solutions of recombined (a) Stx1 and (b) Stx2, at pH 7 and 25 °C.

presence of free B pentamer in Stx1 holotoxin preparations. It should be noted, however, that the recombined holotoxins were found to be somewhat less resistant to acid-induced dissociation compared to native Stx1 and Stx2. The pH_{diss} values for recombined Stx1 and Stx2 were found to be ~4.0 at 37 °C (data not shown). The reason(s) for the lower resistance to acid-induced dissociation of recombined holotoxins is (are) not currently known.

CONCLUSIONS

In summary, the results of the present study provide new insights into the biochemical properties of the Shiga toxins. Direct ES-MS measurements revealed that Stx1 and Stx2 exhibit differences in their resistance to temperature- and acid-induced dissociation. However, both Stx1 and Stx2 are fully assembled at pH > 3.5 and 37 °C. This finding indicates that enzymatic activation of the A subunits of Stx1 and Stx2 involves the intact holotoxins and suggests that the differential toxicities of Stx1 and Stx2 may reflect the relative efficiencies of intracellular activation of the A subunits. Finally, the application of the ES-MS assay to a series of single and double point mutants of the B subunits of Stx1 and Stx2 revealed that the differential stability of their respective homopentamers in solution at pH 7 is due to the presence of a repulsive interaction involving Asp70 of the Stx2 B subunit.

ACKNOWLEDGMENT

The authors thank David Bundle for generously providing the synthetic carbohydrates used in this work.

REFERENCES

1. Karmali, M. A. (2004) Infection by Shiga toxin-producing *Escherichia coli*—an overview. *Mol. Biotechnol. 26*, 117–122.
2. Fraser, M. E., Chernaia, M. M., Kozlov, Y. V., and James, M. N. (1994) Crystal-structure of the holotoxin from shigella-dysenteriae at 2.5-angstrom resolution. *Nat. Struct. Biol. 1*, 59–64.
3. Fraser, M. E., Fujinaga, M., Cherney, M. M., Melton-Celsa, A. R., Twiddy, E. M., O'Brien, A. D., and James, M. N. (2004) Structure of Shiga toxin type 2 (Stx2) from *Escherichia coli* O157:H7. *J. Biol. Chem. 279*, 27511–27517.
4. Calderwood, S. B., Auclair, F., Donohue-Rolfe, A., Keusch, G. T., and Mekalanos, J. J. (1987) Nucleotide-sequence of the Shiga-like toxin genes of *Escherichia coli*. *Proc. Natl. Acad. Sci. U.S.A 84*, 4364–4368.
5. Strockbine, N. A., Jackson, M. P., Sung, L. M., Holmes, R. K., and O'Brien, A. D. (1988) Cloning and sequencing of the genes for Shiga toxin from shigella-dysenteriae type-1. *J. Bacteriol. 170*, 1116–1122.
6. Lingwood, C. A., Law, H., Richardson, S. E., Petric, M., Brunton, G. L., De Grandis, S., and Karmali, M. A. (1987) Glycolipid binding of purified and recombinant *E. coli* produced Verotoxin *in vitro*. *J. Biol. Chem. 262*, 8834–8839.
7. Sandvig, K., Carred, O., Prydz, K., Kozlov, J. V., Hansen, S. H., and van Deurs, B. (1992) Retrograde transport of endocytosed Shiga toxin to the endoplasmic reticulum. *Nature 358*, 510–512.
8. Ogasawara, T., Ito, K., Igarashi, K., Yutsudo, T., and Takeda, Y. (1987) Inhibition of elongation factor 1-dependent aminoacyl-tRNA binding to ribosomes by Shiga-toxin 1 (VT1) from *Escherichia coli* O157:H7 and by Shiga toxin. *FEMS Microbiol. Lett. 44*, 91–94.
9. Schmidt, H., Maier, E., Karch, H., and Benz, R. (1996) Pore-forming properties of the plasmid-encoded hemolysin of enterohemorragic *Escherichia coli* O157:H7. *Eur. J. Biochem. 241*, 594–601.
10. Tesh, V. L., Burris, J. A., Owens, J. W., Gordon, V. M., Wadolkowski, E. A., O'Brien, A. D., and Samuel, J. E. (1993) Comparison of the relative toxicities of Shiga-like toxins type-1 and type-2 for mice. *Infect. Immun. 61*, 3392–3402.
11. Head, S. C., Karmali, M. A., and Lingwood, C. A. (1991) Preparation of Vt1 and Vt2 hybrid toxins from their purified dissociated subunits—evidence for B-subunit modulation of a subunit function. *J. Biol. Chem. 266*, 3617–3621.
12. Kitova, E. N., Kitov, P., Paszkiewicz, E., Kim, J., Mulvey, G. L., Armstrong, G. D., Bundle, D. R., and Klassen, J. S. (2007) Affinities of Shiga toxins 1 and 2 for univalent and oligovalent Pk trisaccharide analogs measured by electrospray ionization mass spectrometry. *Glycobiology 17*, 1127–1137.
13. Brigotti, M., Carnicelli, D., Alvergna, P., Mazzaracchio, R., Sperti, S., and Montanaro, L. (1997) The RNA-N-glycosidase activity of Shiga-like toxin 1: kinetic parameters of the native and activated toxin. *Toxicon 35*, 1431–1437.
14. Kitova, E. N., Daneshfar, R., Marcato, P., Mulvey, G. L., Armstrong, G., and Klassen, J. S. (2005) Stability of the homopentameric B subunits of Shiga toxins 1 and 2 in solution and the gas phase as revealed by nanoelectrospray Fourier transform ion cyclotron resonance mass spectrometry. *J. Am. Soc. Mass Spectrom. 16*, 1957–1968.
15. Loo, J. A. (1997) Studying noncovalent protein complexes by electrospray ionization mass spectrometry. *Mass Spectrom. Rev. 16*, 1–23.
16. Robinson, C. V. (2002) Protein complexes take flight. *Nat. Struct. Biol. 9*, 505–506.
17. Heck, A. J., and Van den Heuvel, R. H. (2004) Investigation of intact protein complexes by mass spectrometry. *Mass Spectrom. Rev. 23*, 368–389.
18. van den Heuvel, R. H., and Heck, A. J. (2004) Native protein mass spectrometry: from intact oligomers to functional machineries. *Curr. Opin. Chem. Biol. 8*, 519–526.
19. Hernandez, H., Dziembowski, A., Taverner, T., Seraphin, B., and Robinsin, C. V. (2006) Subunit architecture of multimeric complexes isolated directly from cells. *EMBO Rep. 7*, 605–610.
20. Synowsky, S. A., van den Heuvel, R. H., Mohammed, S., Pijnappel, P. W., and Heck, A. J. (2006) Probing genuine strong interactions and post-translational modifications in the heterogeneous yeast exosome protein complex. *Mol. Cell. Proteomics 5*, 1581–1592.
21. Kitagawa, N., Mazon, H., Heck, A. J. R., and Wilkens, S. (2008) Stoichiometry of the peripheral stalk subunits E and G of yeast V-1-ATPase determined by mass spectrometry. *J. Biol. Chem. 383*, 3329–3337.
22. Mulvey, G., Vanmaele, R., Mrazek, M., Cahill, M., and Armstrong, G. D. (1998) Affinity purification of Shiga-like toxin I and Shiga-like toxin II. *J. Microbiol. Methods 32*, 247–252.
23. Mulvey, G. L., Marcato, P., Kitov, P. I., Sadowska, J., Bundle, D. R., and Armstrong, G. D. (2003) Assessment in mice of the therapeutic potential of tailored, multivalent Shiga toxin carbohydrate ligands. *J. Infect. Dis. 187*, 640–649.
24. Simpson, R. J. (2003) *Proteins and Proteomics: A Laboratory Manual*, pp 85–86, Cold Spring Harbor Laboratory Press, Cold Spring Harbor, NY.
25. Marcato, P., Mulvey, G., Read, R. J., Van der Helm, K., Nation, P. A., and Armstrong, G. D. (2001) Immunoprophylactic potential of cloned shiga toxin 2 B subunit. *J. Infect. Dis. 183*, 435–443.
26. Daneshfar, R., Kitova, E. N., and Klassen, J. S. (2004) Determination of protein-ligand association thermochemistry using variable-temperature nanoelectrospray mass spectrometry. *J. Am. Chem. Soc. 126*, 4786–4787.
27. Sun, J., Kitova, E. N., and Klassen, J. S. (2007) Method for stabilizing protein-ligand complexes in nanoelectrospray ionization mass spectrometry. *Anal. Chem. 79*, 416–425.
28. Sun, J., Kitova, E. N., Sun, N., and Klassen, J. S. (2007) Method for identifying nonspecific protein-protein interactions in nanoelectrospray ionization mass spectrometry. *Anal. Chem. 79*, 8301–8311.
29. Williams, J. P., Green, B. N., Smith, D. C., Jennings, K. R., Moore, K. A. H., Slade, S. E., Roberts, L. M., and Scrivens, J. H. (2005) Noncovalent Shiga-like toxin assemblies: Characterization by means of mass spectrometry and tandem mass spectrometry. *Biochemistry 44*, 8282–8290.
30. Kitova, E. N., Kitov, P., Bundle, D. R., and Klassen, J. S. (2001) The observation of multivalent complexes of the Shiga-like toxin with globotriaoside and the determination of their stoichiometry by nanoelectrospray Fourier-transform ion cyclotron resonance mass spectrometry. *Glycobiology 11*, 605–611.
31. Dobo, A., and Kaltashov, E. A. (2001) Detection of multiple protein conformational ensembles in solution via deconvolution of charge-state distributions in ESI MS. *Anal. Chem. 73*, 4763–4773.
32. Recchi, C., and Chavrier, P. (2006) V-ATPase: a potential pH sensor. *Nat. Cell Biol. 8*, 107–109.
33. Wang, W., Kitova, E. N., and Klassen, J. S. (2003) Influence of solution and gas phase processes on protein-carbohydrate binding affinities determined by nanoelectrospray Fourier transform ion cyclotron resonance mass spectrometry. *Anal. Chem. 75*, 4945–4955.